Numerical Analysis of Fluid Behavior for Cerium Oxide in Back Ward Facing Step Problem

[1]Miss. PallaviGola, [2]Mr. Anandkumar S Malipatil,

1. PG Student Department of Thermal Power Engineering (MTP) Visvesvaraya Technological University, Postgraduate Centre, Regional Office, Kalaburagi 585105

2. Assistant Professor Department of Thermal Power Engineering (MTP) Visvesvaraya Technological University, Postgraduate Centre, Regional Office, Kalaburagi 585105.

Abstract

The flow separation and reattachment of the fluid is one of the common phenomena that happen in many engineering applications. Backward facing step geometry, where the flow separation happens due to a sudden expansion is one of the structures that can be found in heating and cooling devices such as: nuclear reactors, combustion chambers, flow in valves, cooling compressors blade, electronic cooling equipment, wide angle diffusers, and high-performance heat exchangers. The separation of the flow is unwanted in many of the previous examples due to the pressure drop, which causes energy losses by the additional fan or pumping power. However, in some applications for instance in the burner flame stabilization, the flow separation can enhance the heat transfer, where it is used for turbulence promotion.

In this Project a Next generation nanofluid is Taken to analyze the fluid behavior using back ward facing Step a homogenous Mixture is taken to analysis using computational fluid dynamics with cerium oxide in a laminar flow condition with Reynolds number between 10 to 400 different volume fractions of the nano fluid is considered and analyzed during the Simulation and compared.

Keywords : CFD, Cerium Oxide, Homogenous Mixture , Back ward Step.

I. INTRODUCTION

One of the important engineering applications, where the fluid flows through unexpected bends and encounters sudden expansions is the 'air filter housings' of automobiles. The bends and encounters sudden expansions is the 'air filter housings' of automobiles. The rationale behind this complex flow path in present day automobiles is that the design criteria are determined by space utilization rather than fluid mechanics. This arrangement results in the flow being non-uniform and the mean velocity of the flow is not normal to the surface of the filter. Moreover, the velocity fluctuations observed in the separation region combined with non-uniform flow are found to be detrimental to the performance of the filter.

Previous research has shown that the velocity fluctuations and non-uniform flow through the filter are the important factors on which the filtration efficiency depends. The real flow field through air filter housing, when considered with all its geometrical parameters is extremely intricate and expensive to simulate numerically. Also, it is not feasible to measure all the minute details of the real flow field. Thus, the need to build a simplified model of this complex flow that will result in a better understanding of the interaction between the separation region and the porous medium is highlighted in this research. For some engineering applications, the above phenomena (separation and re-attachment) facilitates in enhancing the momentum, heat and/or mass transfer rates while for the others, it may lead to an unsteady flow resulting in noise, vibration and reduced efficiency. Other significant applications of flow modeling through porous media can be found in designs of fluidized bed combustors, catalytic reactors, crude-oil drilling, flows in the core of nuclear reactors and environmental flows over forests and vegetation. Hence, turbulent flow modeling in porous media is an essential exercise in understanding various complex engineering and environmental flows.

1.2 Backward Facing Step

The backward-facing step flow (see Figure 1-1) is a fundamental flow that provides a simple geometry to serve as a prototype for studying complex phenomena like flow separation and re-attachment. It is similar to many industrial flows, including housings for automotive air filters and headers for compact cross flow heat exchangers. A comprehensive understanding of these phenomena is of prime importance for the design of engineering devices like diffusers, turbines, combustors, airfoils, etc.

Figure 1.1 shows a two-dimensional schematic of a backward facing step with a porous insert. The channel height is denoted by's' and step-height is denoted by 'h'. The expansion ratio (ER) is then defined as shown in Equation.

$$RE=S/S+H$$

In the present study the step-flow experiments of Armaly et al. (1983) and Yao

(2000) were modeled using commercial software FLUENT and the mesh was created using pre-processing software GAMBIT. Table I details the geometries of the two experimental studies examined in the present study.

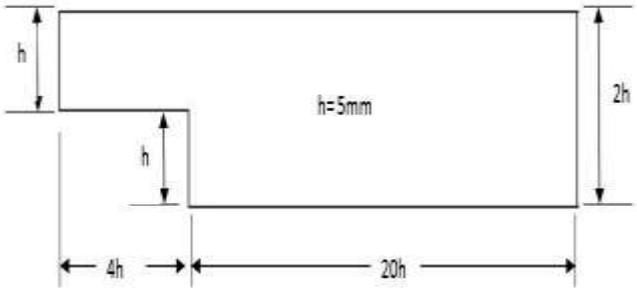

Figure 1 Geometry Description

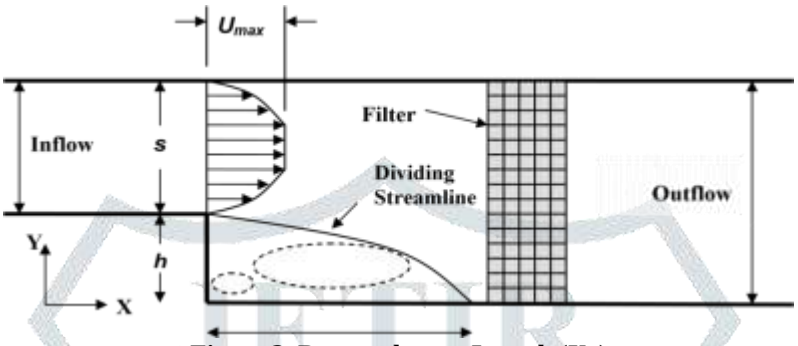

Figure 2 Re-attachment Length (X_R)

II. LITERATURE REVIEW

The backward-facing step flow was already of interest even when fluid mechanical problems used to be addressed only by potential flow theory. As shown by Lee and Smith, potential flow theory permits the treatment of the backward-facing step flow yielding a streamline pattern which does not indicate any separation or recirculation region behind the step. Hence potential theory does not provide the generally expected separation of the flow at the upper corner of the step, nor does the lower corner yield a region of vortices as expected from the considerations of Moffatt.

Moffatt predicted under specified conditions the existence of a sequence of vortices near corners as shown in Fig. 1 for ReD→0. Early numerical predictions of backward-facing step flows, see, e.g., Roache, Taylor and Ndefo.

Durst and Pereira, did not show any separation at the upper corner of the step for low Reynolds numbers. However, a separated region was predicted at the lower corner that contained a single vortex only. A careful analysis of the flow in sudden expansions was carried out by

Alleborn et al. and it was indicated that, at least at low Reynolds numbers, the lower corner contains a sequence of Moffatt vortices. It was concluded by Alleborn et al. that the earlier numerical predictions were carried out with insufficient numerical grid resolution to resolve the smaller vortices at the lower corner.

Hence high-performance computers are needed to carry out detailed studies of backward-facing step flows, even at low Reynolds numbers. Furthermore, since the early work to predict the backward-facing step flows, new numerical methodologies such as the multigrid method see, e.g., Brandt et al., Hackbusch or local block refinement see, e.g., Lange et al. have been introduced into computer programs for solving the Navier-Stokes equations more efficiently with a faster convergence rate.

Among literatures some of researchers have focused on installation of barrier or blockage shape in the way of flow. Cheng et al. investigated the influence of the forced convection characteristics of backward facing step flow numerically in a 2D duct through the inserting of slotted and solid baffles onto the duct wall. They found that a slotted baffle can increase the average Nusselt number by the maximum 190%.

III. METHODOLOGY

The geometry is developed based on the step size. An expansion ratio of 1:2 is assumed during the development of geometry. Other parameters are assumed as a function of h. Figure 1 shows the schematic of the geometry of a backward facing step. The step size is assumed a 5mm. To predict accurate flow behavior the downstream domain is assumed 20 times longer than the step.

The computational domain is schematically shown in Figure 1. The expansion ratio has been chosen as H/h=1.9432, and the length of the upstream wall, and downstream were Lu = 5 m, and Ld =10 m, respectively. The flow at the inlet was considered to be hydrodynamically steady with temperature of 274 K and the velocity specified by Reynolds number $10 \leqslant Re \leqslant 400$. The downstream stepped wall was heated with constant temperature of 400 K, and all the other walls were fixed to be adiabatic. The single-phase approach for solving the flow of nanofluid problem is adopted in this numerical study. In this approach the following assumptions are used: The nanoparticles and the base fluid (water) are to be perfectly mixed and treated as a homogenous mixture. Moreover, the fluid phase and the solid particles are assumed to be in thermal equilibrium and move with the same velocity. Steady, Newtonian and incompressible fluid flow is considered. The thermophysical properties of the nanofluid are temperature independent and assumed to be dependent on the volume fraction of the nanoparticles.

3.1 Governing equations

Equations (1) to (3) are continuity, momentum, and energy governing equations that present the mathematical formulation of the single-phase model.

$$div(\rho_{nf}\vec{V}) = 0 \quad (1)$$

$$div(\rho_{nf}\vec{V}\vec{V}) = -\nabla P + \mu_{nf}\nabla^2\vec{V} \quad (2)$$

$$div(\rho_{nf}\vec{V}C_{pnf}T) = div(k_{nf}\nabla T) \quad (3)$$

where the following notations are used:

$\vec{V}$, P, and T present the velocity vector, pressure, and temperature, respectively. $\mu_{nf}$is the viscosity of nanofluid,$\rho_{nf}$is density of the nanofluid, k_{nf}, and C_{pnf} are the thermal conductivity and thermal capacity, respectively.

3.2 Thermal properties of the nanofluid

The thermal properties of the nanofluid are modelled as a function of the volume fraction. The viscosity, density, thermal capacity, and the thermal conductivity are approximated depending on the concentration of the nanoparticles in the base fluid using equation (4)-(7) as defined in. Table 1. Shows the thermo-physical properties for Al_2O_3-water at a different values of ϕ.

$$\mu_{nf} = \frac{\mu_b}{(1-\phi)^{2.5}} \quad (4)$$

$$\rho_{nf} = (1-\phi)\rho_b + \phi_p\rho_p, \quad (5)$$

$$C_{pnf} = \frac{\phi(\rho C_p)_p + (1-\phi)(\rho C_p)_b}{\rho_{nf}}, \quad (6)$$

$$k_{nf} = k_b \frac{k_p + 2k_b - 2\phi(k_b - k_p)}{k_p + 2k_b + \phi(k_b - k_p)}. \quad (7)$$

Table 1. The thermo-physical properties of water-Al2O3 at different value of ϕ

Parameter	Pure water (0%)	Al_2O_3-water (1%)	Al_2O_3-water (2%)	Al_2O_3-water (3%)	Al_2O_3-water (4%)
$\rho[kg/m^3]$	997.1	1026.829	1056.558	1086.287	1116.016
$C_p[J/kg.K]$	4179	4047.005	3922.4389	3804.6906	3693.2155
k|w/m.K|	0.613	0.63073914	0.6488238	0.6672642	0.6860711
μ[Pa.s]	0.001	0.001025444	0.001051180	0.001079122	0.001107444

Geometry

The geometry is generated by using ICEM CFD, and the two-dimensional flow problem was chosen according to the experimental setup published by Armaly et al [3], where H/h=1.9432 is the expansion ratio. H is the channel height downstream, and h is the height of the inflow channel. In the present study, all the geometrical length is made based on the channel height, Lu =5h is the upstream channel length, while Ld=10 h is the downstream channel length.

3.2. Mesh grid testing and model validation

Non-uniform quadrilateral grid system is employed for meshing the domain generated by Blocking method in ICEM CFD as shown in Figure 4. The grid is centred on the walls and the step will give greater simulation accuracy and more efficient computing time. The maximum face size of the mesh was 0.005 m and the maximum aspect ratio 1:2. Four different meshes represent the criteria of grid independency at Re=100 (see Table 1).

The purpose of this mesh dependency study for X1 is to avoid the result relying on the mesh. After the 3rd mesh, the grid difference is less than 1%, which can be considered as grid-independent. For further validation, the result of the reattachment point compared to Armaly's work, where the result showed excellent agreement, as shown in Figure 3.

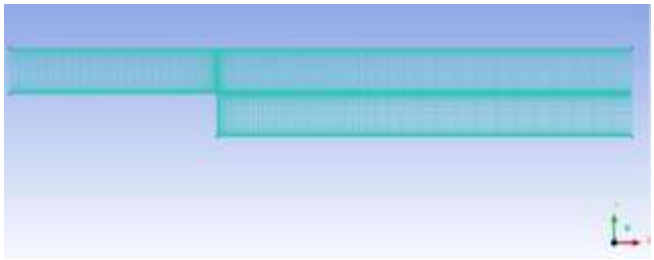

Figure 2. Mesh generation for the model

Table 2. The grid independency

Mesh	Size	X1
1	25*80	2.6891
2	35*90	2.7078
3	40*100	2.7191
4	50*110	2.7192

3.3 Numerical solution method

A finite volume method (FVM) was used for discretizing the equations of mass, momentum, and energy. ANSYS fluent solver used to perform the calculations by solving the system of equations (1) – (3) together with the boundary conditions. The solution method was as follows: a simple algorithm was used to resolve the velocity-pressure coupling. The convection and diffusion terms in the governing equations were discretized using a second-order upwind scheme. The convergence criteria of the solutions monitored by a residual monitor of 10-6.

VALIDATION CASE

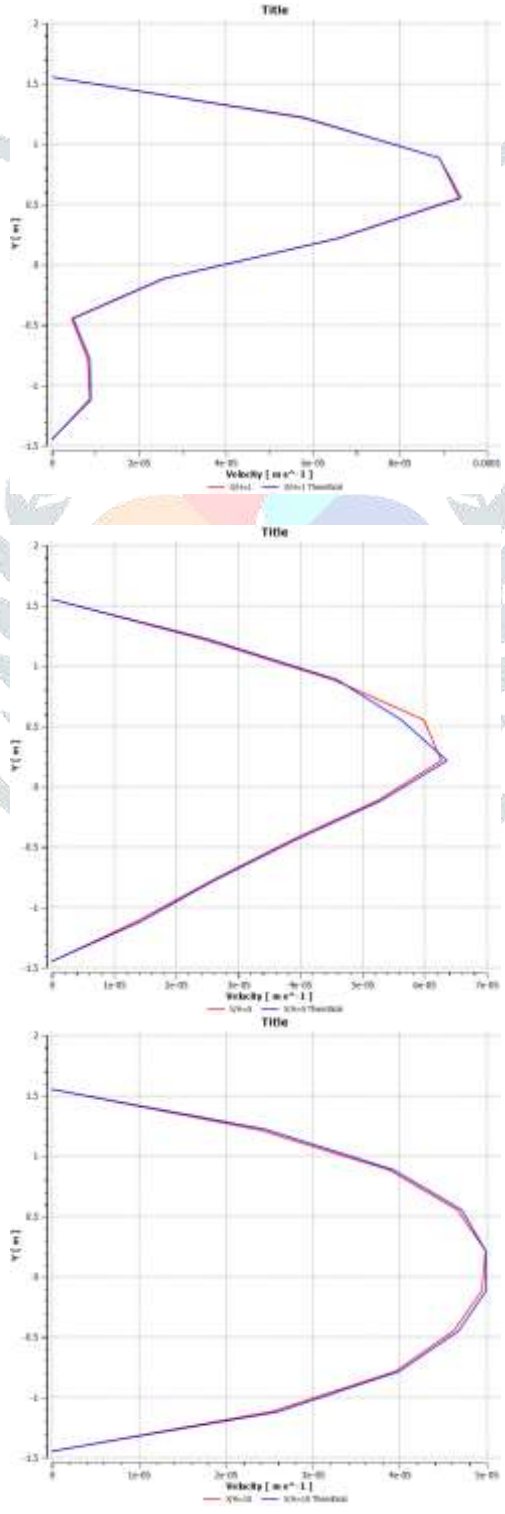

IV. RESULTS & DISCUSSION

4.1 Hydrodynamic effect of nanofluid

The distributions of the velocity for different nanoparticle volume fractions for Re=100 and at different sections along the downstream channel are shown in Figures 8-10 for volume fraction ϕ=1, 3, or 45%. The numerical simulations show that the velocity increases as the volume fraction increase at the location x=5, and after the reattachment point the velocity starts to decrease as the volume fraction increases. Two observations are made for the velocity distribution along the downstream wall. The first is for the area between the side wall and the reattachment point, where the result shows that the velocity of the nanoparticles is independent from the sudden expansion and was influenced by the volume fraction, where the velocity increase as the concentration of the particles in the base fluid increases. The second observation after the recirculation zone is that the velocity starts to decrease as the volume fraction increases and that can be seen in at the outlet x=10, and that is shown in below fig at the outlet x=10.

Case 1 Backward step with Water

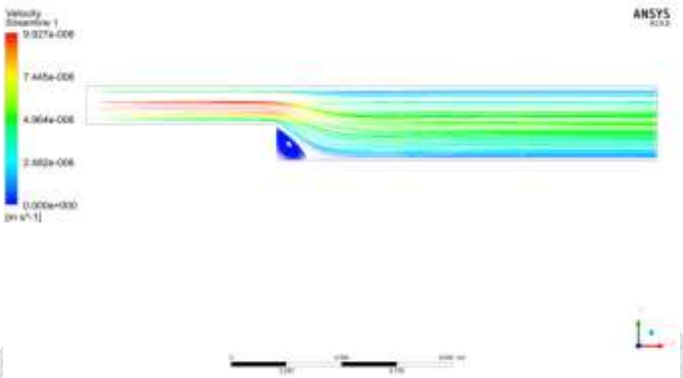

Fig 4.1 Stream Lines Generated for Re=10 with Water.

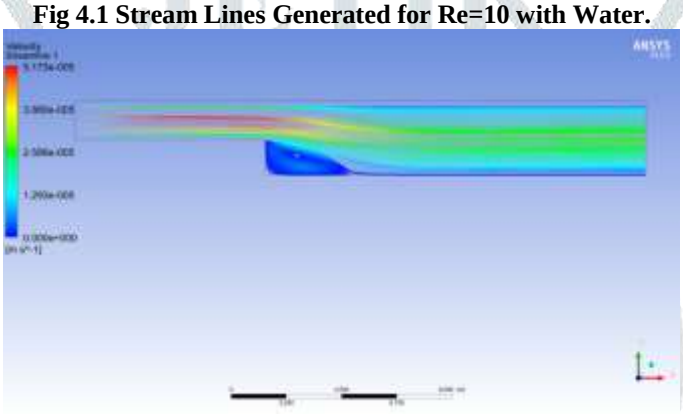

Fig 4.2 Stream Lines Generated for Re=50 with Water.

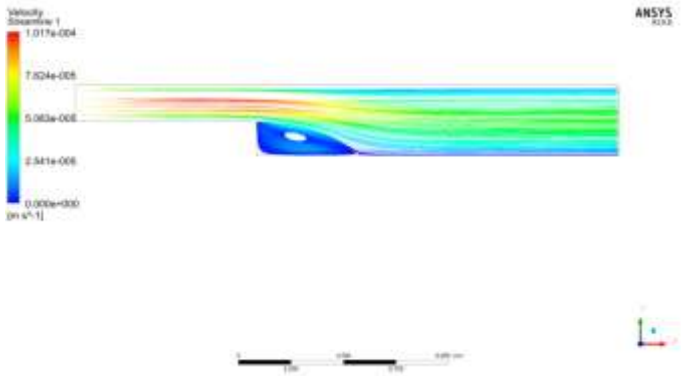

Fig 4.3 Stream Lines Generated for Re=100 with Water.

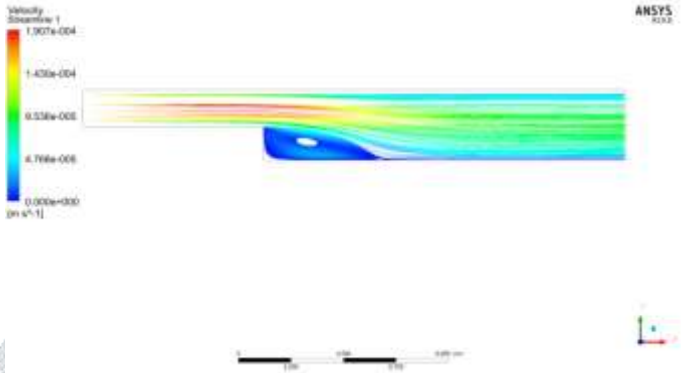

Fig 4.4 Stream Lines Generated for Re=200 with Water.

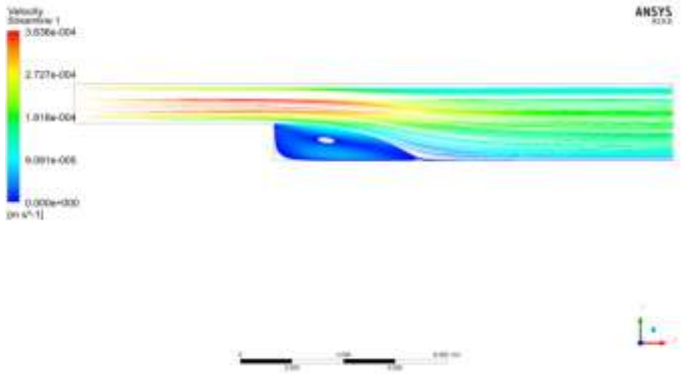

Fig 4.5 Stream Lines Generated for Re=400 with Water.

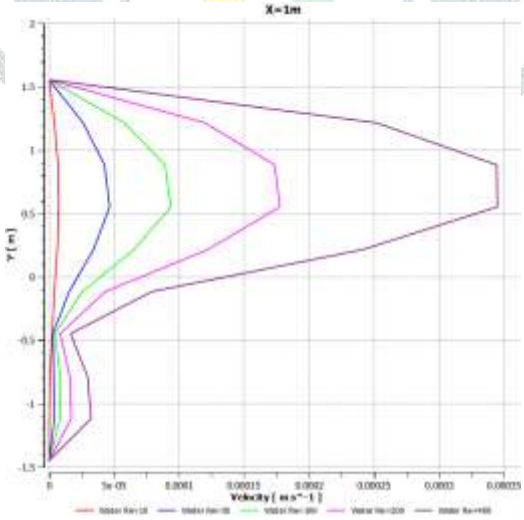

Plot 1 Velocity Profile For X=1 m at Re=10-400

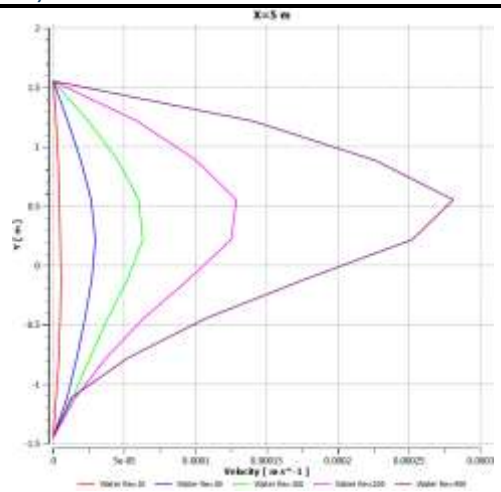

Plot 2 Velocity Profile For X=5 m at Re=10-400.

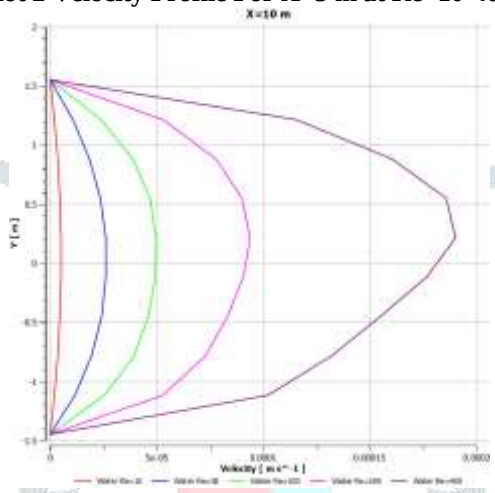

Plot 3 Velocity Profile For X=10 m at Re=10-400.

Case 2 Backward step with Cerium Oxide 1%

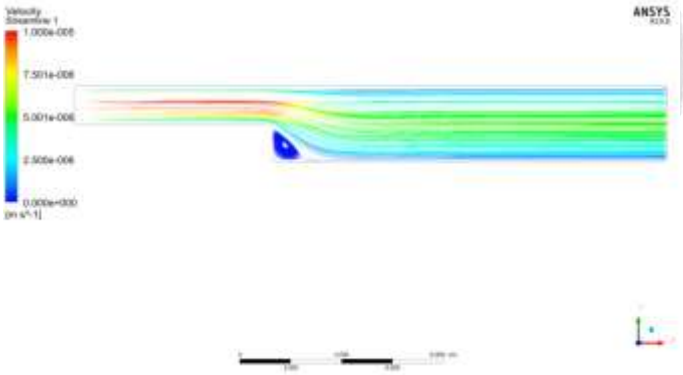

Fig 4.6 Stream Lines Generated for Re=10 with Ce2o3.

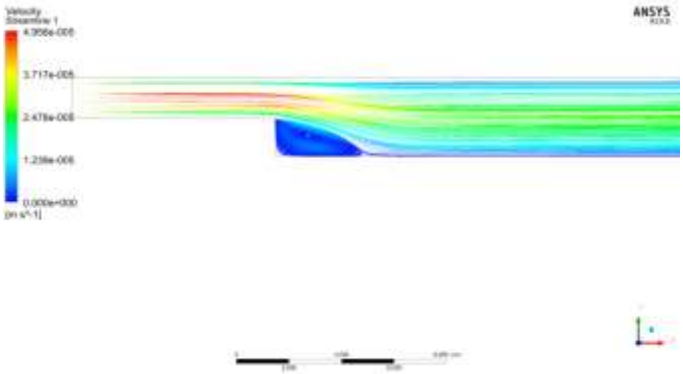

Fig 4.7 Stream Lines Generated for Re=50 with Ce2o3.

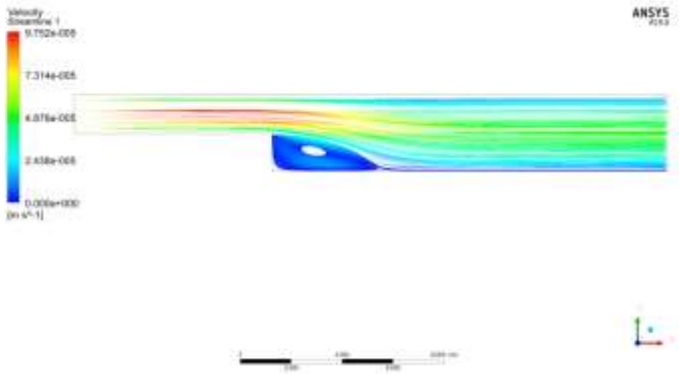

Fig 4.8 Stream Lines Generated for Re=100 with Ce2o3.

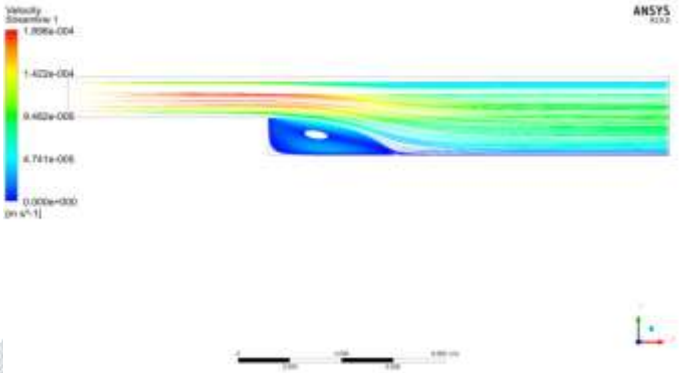

Fig 4.9 Stream Lines Generated for Re=200 with Ce2o3.

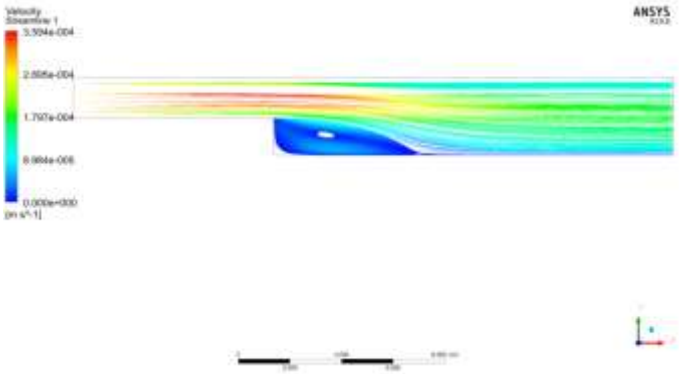

Fig 4.10 Stream Lines Generated for Re=400 with Ce2o3.

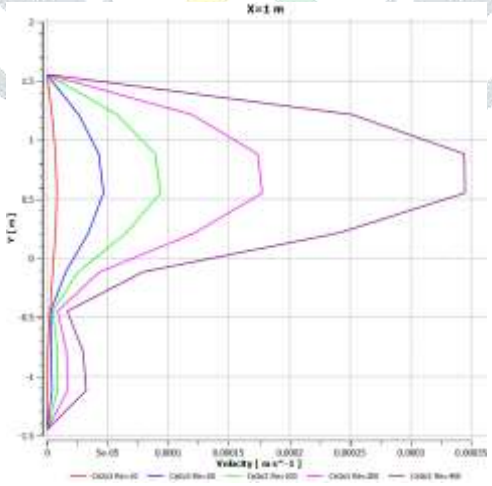

Plot 4 Velocity Profile For X=1 m at Re=10-400 Ce2o3 1%

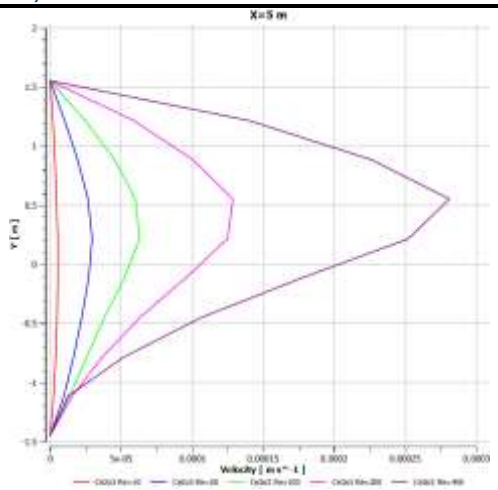

Plot 5 Velocity Profile For X=5 m at Re=10-400 Ce2o3 1%

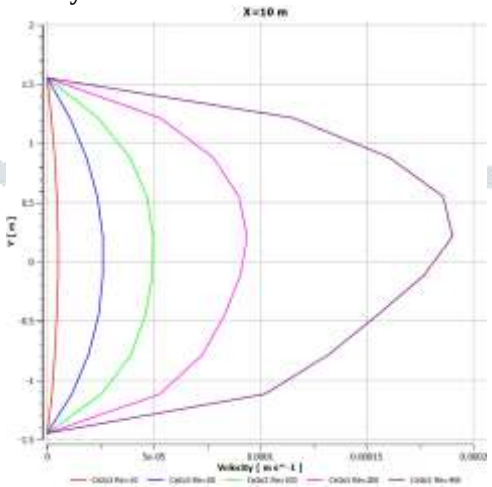

Plot 6 Velocity Profile For X=10 m at Re=10-400 Ce2o3 1%

Case 3 Backward step with Cerium Oxide 3%

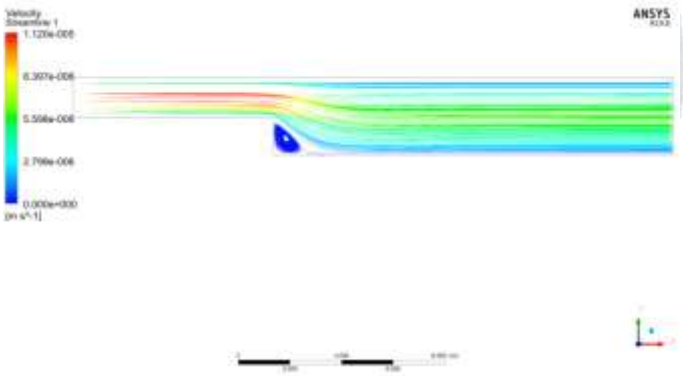

Fig 4.11 Stream Lines Generated for Re=10 with Ce2o3.

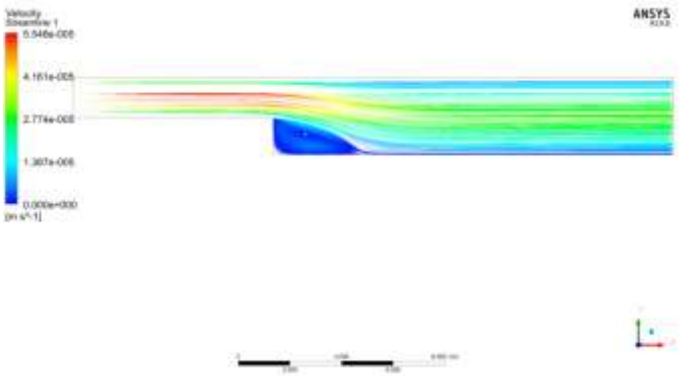

Fig 4.12 Stream Lines Generated for Re=50 with Ce2o3.

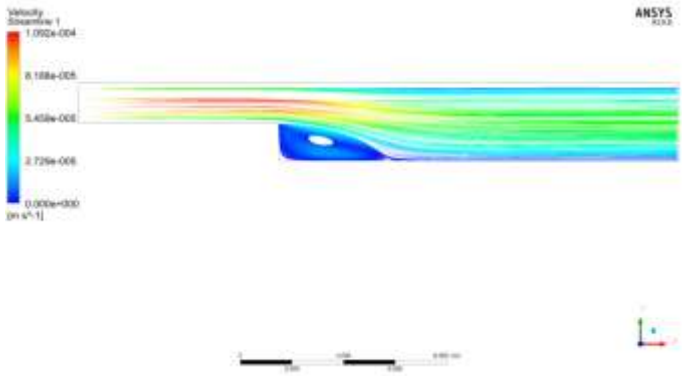

Fig 4.13 Stream Lines Generated for Re=100 with Ce2o3.

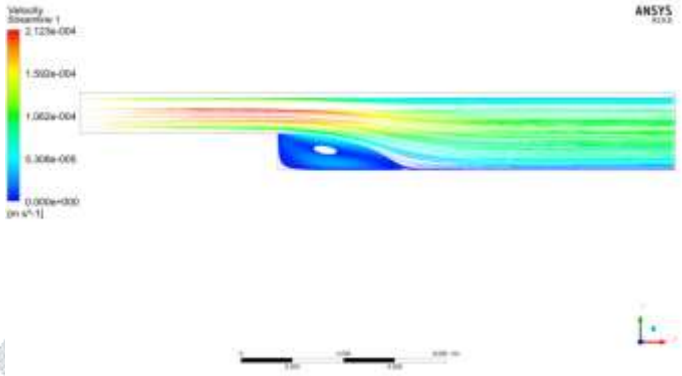

Fig 4.14 Stream Lines Generated for Re=200 with Ce2o3.

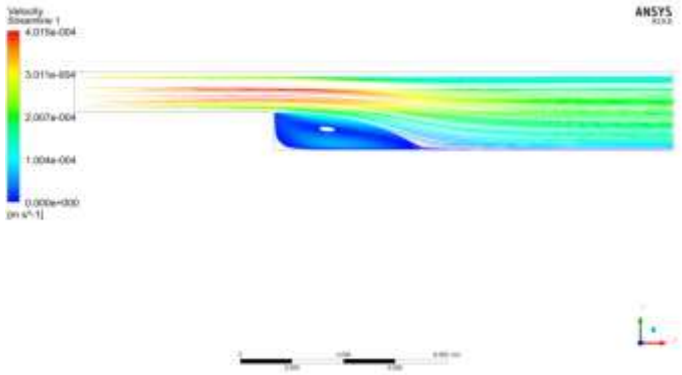

Fig 4.15 Stream Lines Generated for Re=400 with Ce2o3.

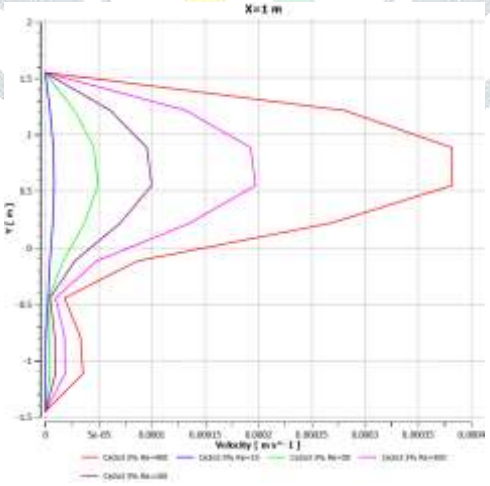

Plot 7 Velocity Profile For X=1 m at Re=10-400 Ce2o3 1%

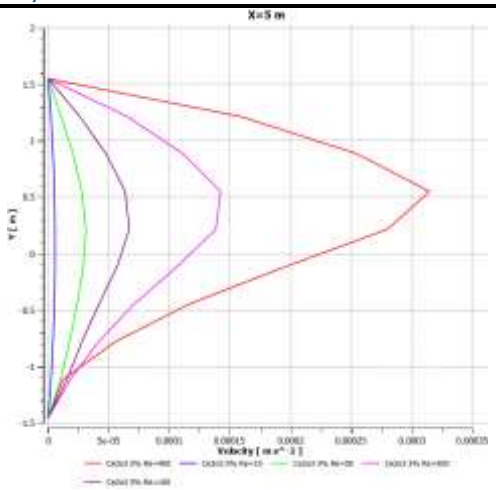

Plot 8 Velocity Profile For X=5 m at Re=10-400 Ce2o3 3%

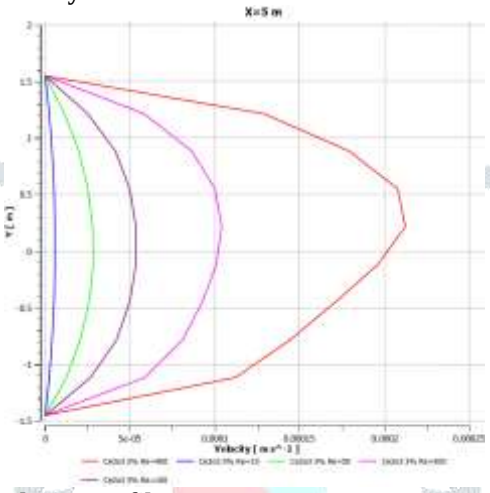

Plot 9 Velocity Profile For X=10 m at Re=10-400 Ce2o3 %

Case 4 Backward step with Cerium Oxide 3=5%

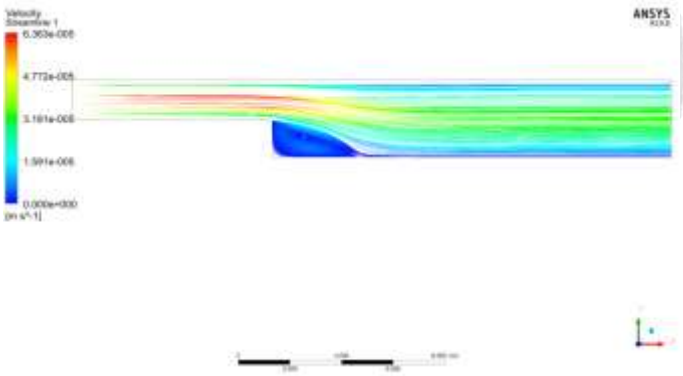

Fig 4.16 Stream Lines Generated for Re=10 with Ce2o3.

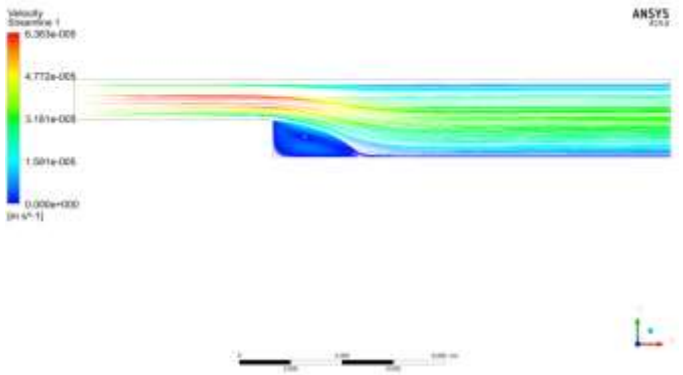

Fig 4.17 Stream Lines Generated for Re=50 with Ce2o3.

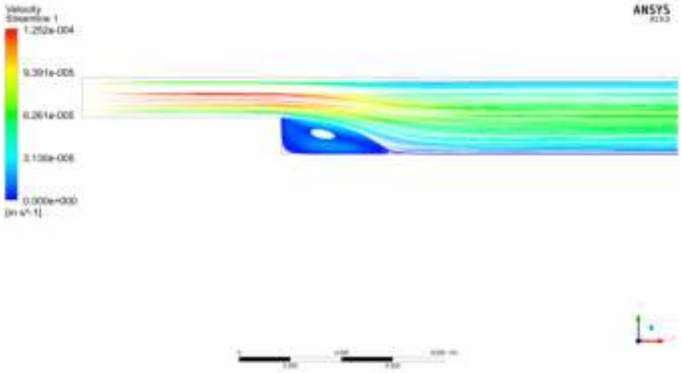

Fig 4.18 Stream Lines Generated for Re=100 with Ce2o3.

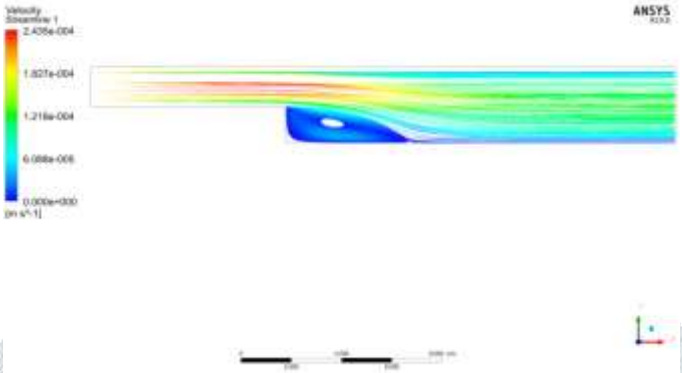

Fig 4.19 Stream Lines Generated for Re=200 with Ce2o3.

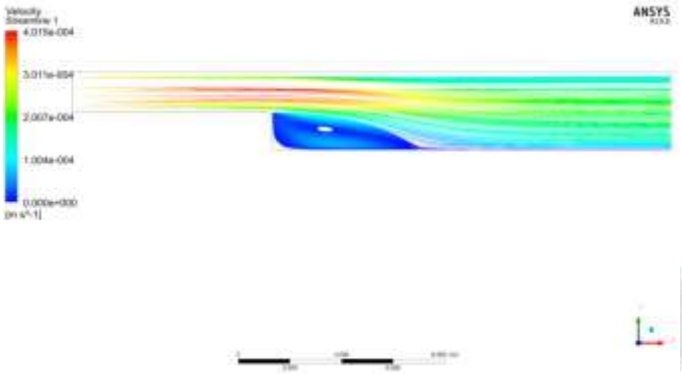

Fig 4.20 Stream Lines Generated for Re=400 with Ce2o3.

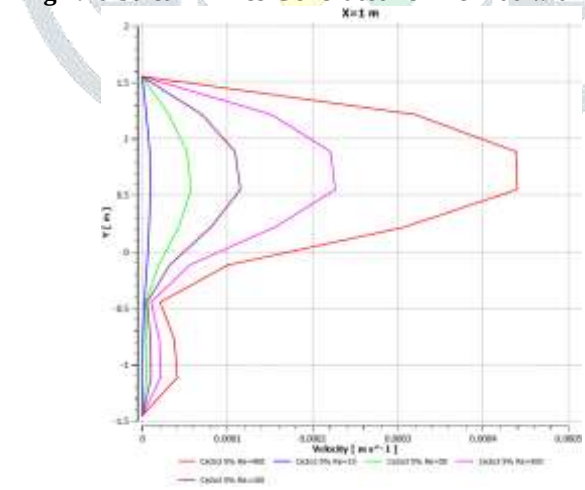

Plot 10 Velocity Profile For X=1 m at Re=10-400 Ce2o3 1%

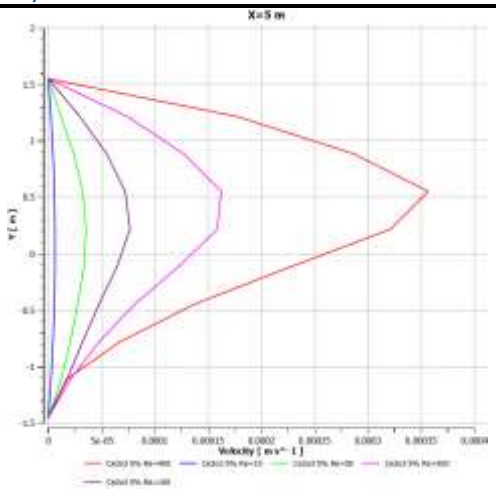

Plot 11 Velocity Profile For X=5 m at Re=10-400 Ce2o3 5%

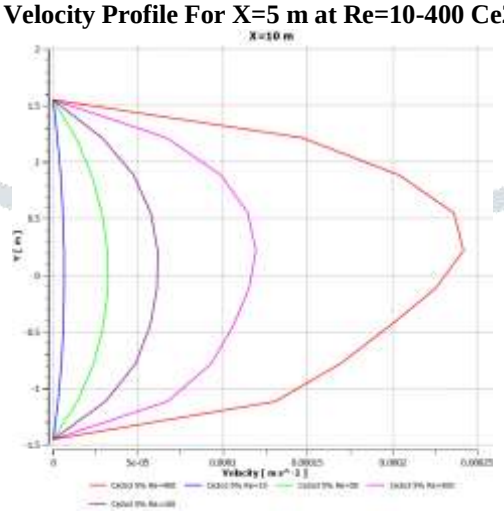

Plot 12 Velocity Profile For X=10 m at Re=10-400 Ce2o3 5%

V. CONCLUSION

CFD simulations of the forced convection flow over backward facing step were carried out. We can summarize our findings as follows:

The flow reattachment points calculated in this paper have excellent agreement with those obtained experimentally by Armaly et al. We have an excellent agreement with result got simulation by Biswas et al. Validating the numerical result with measured data given in. In our paper we have pointed on the impact of the Ce2O3, the temperature distribution and the heat transfer change with volume fraction of the nanoparticles. The maximum velocity shows an increase with increasing volume fraction at x=2, however at the outlet the impact of ϕ is opposite. It is obtained that the temperature is increased with increasing the volume fraction of Ce2O3 everywhere. The heat transfer is higher when the volume fraction is bigger. For the downstream wall, the highest heat transfer performance was obtained for maximal ϕ of tested fluids. Our aim is to investigate the impact of the nanoparticle's material on the velocity and thermal profiles.

REFERENCES

1. Lee, Y. S. and Smith, L. C., 1986, Analysis of power-law viscous materials using complex stream, potential and stress functions, in Encyclopedia of Fluid Mechanics, vol. 1, Flow Phenomena and Measurement, ed. N. P. Cheremisinoff, pp. 1105–1154.
2. Moffatt, H. K., 1964, Viscous and resistive eddies near a sharp corner, J. Fluid Mech., 18, pp. 1–1
3. Roache, P. J., 1972, Computational Fluid Dynamics, Hermosa, New Mexico, pp. 139–173.
4. Taylor, T. D., and Ndefo, E., 1971, Computation of viscous flow in a channel by the method of splitting, Proc. of the Second Int. Conf. on Num. Methods in Fluid Dynamics, Lecture Notes in Physics, vol. 8, pp. 356–364, Springer Verlag, New York.
5. Durst, F., and Peireira, J. C. F., 1988, Time-dependent laminar backwardfacing step flow in a two-dimensional duct, ASME J. Fluids Eng., 110, pp. 289–296.
6. Alleborn, N., Nandakumar, K., Raszillier, H., and Durst, F., 1997, Further contributions on the two-dimensional flow in a sudden expansion, J. Fluid Mech., 330, pp. 169–188.
7. Brandt, A., Dendy, J. E., and Ruppel, H., 1980, Themultigrid method for semi-implicit hydrodynamic codes, J. Comput. Phys., 34, pp. 348–370.
8. Hackbusch, W., 1985, Multigrid Methods for Applications, Springer, Berlin.
9. Lange, C. F., Scha¨fer, M., and Durst, F., 2002, Local block refinement with a multigrid flow solver, Int. J. Numer. Methods Fluids 38, pp. 21–41.
10. Ladeve´ze, J., and Peyret, R., 1974, Calculnumeriqued'une solution avec singularite´ des equations de Navier-Stokes: e´coulementdans un canal avec variation brusque de section, J. Mech., 13, no. 3, pp. 367–396.
11. Armaly, B. F., Durst, F., Peireira, J. C. F., Scho¨nung, B., 1983, Experimental and theoretical investigation of backward-facing step flow, J. Fluid Mech., 127, pp. 473–496.
12. Durst, F., and Peireira, J. C. F., and Tropea, C., 1993, The plane symmetric sudden-expansion flow at low Reynolds numbers, J. Fluid Mech., 248, pp. 567–581

13. Al-Aswadi, A., H. Mohammed, N. Shuaib and A. Campo, Laminar forced convection flow over a backward facing step using nanofluids. International Communications in Heat and Mass Transfer, 2010. 37(8): p. 950-957.
14. Barrios-Pina, H., S. Viazzo and C. Rey, A numerical study of laminar and transitional mixed convection flow over a backward-facing step. Computers & Fluids, 2012. 56: p. 7791.
15. Kherbeet, A.S., H. Mohammed and B. Salman, The effect of nanofluids flow on mixed convection heat transfer over microscale backward-facing step. International Journal of Heat and Mass Transfer, 2012. 55(21-22): p. 5870-5881.
16. Lan, H., B. Armaly and J. Drallmeier, Three-dimensional simulation of turbulent forced convection in a duct with backward-facing step. International Journal of Heat and Mass Transfer, 2009. 52(7-8): p. 1690-1700.
17. Cheng, J.-C. and Y.-L. Tsay, Effects of solid and slotted baffles on the convection characteristics of backward-facing step flow in a channel. Heat and mass transfer, 2006. 42(9): p. 843-852.
18. Fathinia, F., A. Heshmati, M. Parsazadeh, M.A. Wahid and M.M. Sies. The Influence of Various Inlet Geometries on Mixed Convection Flow of Ethylene Glycol in a Backward Facing Step.in Applied Mechanics and Materials. 2013. Trans Tech Publ.
19. Kumar, A. and A.K. Dhiman, Effect of a circular cylinder on separated forced convection at a backward-facing step. International Journal of Thermal Sciences, 2012. 52: p. 176-185.
20. Nie, J.H., Y. Chen and H.-T. Hsieh, Effects of a baffle on separated convection flow adjacent to backward-facing step. International Journal of Thermal Sciences, 2009. 48(3): p. 618-625.